Acta Biomaterialia 8 (2012) 608–618

Contents lists available at SciVerse ScienceDirect

Acta Biomaterialia

journal homepage: www.elsevier.com/locate/actabiomat

A substrate-independent method for surface grafting polymer layers by atom transfer radical polymerization: Reduction of protein adsorption

Bryan R. Coad [a,b,*], Yi Lu [a], Laurence Meagher [a,b]

[a] CSIRO Materials Science and Engineering, Clayton, 3168 Victoria, Australia
[b] Cooperative Research Centre for Polymers, Notting Hill, 3168 Victoria, Australia

ARTICLE INFO

Article history:
Received 14 June 2011
Received in revised form 31 August 2011
Accepted 5 October 2011
Available online 11 October 2011

Keywords:
Biomaterial interface engineering
Surface-initiated ATRP
Polymer brush
Low-fouling biomaterials

ABSTRACT

A general method for producing low-fouling biomaterials on any surface by surface-initiated grafting of polymer brushes is presented. Our procedure uses radiofrequency glow discharge thin film deposition followed by macro-initiator coupling and then surface-initiated atom transfer radical polymerization (SI-ATRP) to prepare neutral polymer brushes on planar substrates. Coatings were produced on substrates with variable interfacial composition and mechanical properties such as hard inorganic/metal substrates (silicon and gold) or flexible (perfluorinated poly(ethylene-co-propylene) film) and rigid (microtitre plates) polymeric materials. First, surfaces were functionalized via deposition of an allylamine plasma polymer thin film followed by covalent coupling of a macro-initiator composed partly of ATRP initiator groups. Successful grafting of a hydrophilic polymer layer was achieved by SI-ATRP of *N*,*N*′-dimethylacrylamide in aqueous media at room temperature. We exemplified how this method could be used to create surface coatings with significantly reduced protein adsorption on different material substrates. Protein binding experiments using labelled human serum albumin on grafted materials resulted in quantitative evidence for low-fouling compared to control surfaces.

1. Introduction

Surface-initiated atom transfer radical polymerization (SI-ATRP) has great potential for beneficially altering the surface properties of materials [1–4]. This is particularly important for new biomedical materials, which are chosen for their suitable bulk material properties but often require modification of their surface properties. Along with other controlled/living radical polymerization techniques, SI-ATRP can decorate a surface with dense polymer brush layers with substantially different physical and chemical properties to the bulk material and can be easily tailored by the use of different monomers to generate homopolymers, statistical copolymers or block copolymers [1,5,6]. SI-ATRP has shown wide applicability on a variety of substrates, including silicon [7–13], gold [14], glass [15–17], stainless steel [18], mica [19] and polymeric substrates [20–23]. The versatility is best illustrated by examining a few of the applications of SI-ATRP. For example, in biological applications SI-ATRP has been used to direct cellular [24] or protein response [25–31] on surfaces such as titanium [32], paper [33], polystyrene latex [34–36], poly (ether ether ketone) [37] and cryogels [38]. In membrane science, SI-ATRP has been used for the surface modification of filters and membranes composed of polycarbonate [39], nylon [40], porous alumina [41] and fluorinated nanofibres [42], as well as molecular transport through silica-based colloidal films [43]. Finally, in separation science, SI-ATRP has been used as a modifier of chromatographic stationary phases, including silica beads [44,45], capillaries [46,47] and beaded polymeric stationary phases [48–50].

Particularly for biomaterials today there is a need for a new class of materials having surface coatings providing some form or function but which are grafted from a host of different bulk materials. For example, in the case where surface coatings are designed to resist adsorption of biomolecules on medical implants, one may wish to have the same effective protein-resistant coating on a hard surface as on a flexible, polymeric one [51]. In other words, because of the great variety of surface chemistries associated with different biomaterials, there is a necessity to develop a cross-platform, substrate-independent grafting protocol for surface modification. Most materials grafted by SI-ATRP rely in some way upon initiator immobilization through thiol or silane linkages because gold and silicon are typical model substrates. However, deposition methods are more ideally geared toward developing a platform technology for coating many types of materials with ATRP initiators. Some notable examples include the investigation by Jiang et al. using vapor deposition of an initiator [52]. Also, Teare et al. have investigated a substrate-independent grafting methodology using a pulsed plasma

* Corresponding author. Present address: Ian Wark Research Institute/Mawson Institute, University of South Australia, Mawson Lakes, 5095 South Australia, Australia. Tel.: +61 8 8302 3152; fax: +61 8 8302 3683.
E-mail address: Bryan.Coad@unisa.edu.au (B.R. Coad).

1742-7061/$ - see front matter
doi:10.1016/j.actbio.2011.10.006

technique for uncontrolled polymerizations and demonstrated protein resistance for coatings from poly-*N*-acryloylsarcosine methyl ester [53] and poly(*N*-isopropylacrylamide) [54]. The pulsed plasma technique for immobilization of initiators for grafting by controlled polymerization methods (TEMPO [55] or ATRP [56]) has also been shown; however, the biological response on surfaces coated with controlled polymerization techniques was not measured.

Unlike direct immobilization of small-molecule initiators onto surfaces, immobilization of macro-initiators confers many advantages for SI-ATRP [57]. Macro-initiators tend to be larger molecules (often small molecular weight polymers themselves) composed of surface-anchoring groups and initiating groups. The type of anchoring groups are complementary towards the intended substrate, and charged macro-initiators are ideal for electrostatic adsorption on hard-to-functionalize surfaces such as cationic [58] and anionic sols [59]. Covalent attachment of an ATRP macro-initiator by ultraviolet-linking phenyl azide anchoring groups onto polymeric substrates is also possible [23]. Polymeric macro-initiators are highly customizable (synthesized with variable quantities of initiating groups or indeed, different classes of initiators altogether) and their composition can be determined by nuclear magnetic resonance imaging (NMR). Enormous versatility using the macro-initiator approach was the subject of a platform technology described for immobilization of different controlled radical polymerization initiators (iniferters, reversible addition-fragmentation chain transfer (RAFT) agents and ATRP initiators), leading to well-defined polymer layers grafted from substrates using a variety of surface-initiated controlled radical polymerization techniques [60]. Here, the initial surface coverage of a covalently attached plasma polymer coating complementary to the anchoring groups present on the macro-initiator allows a near limitless array of substrates to be covalently functionalized by controlled radical polymerization techniques.

In this paper, we demonstrate a cross-platform methodology to graft polymers from substrates representing diverse classes of materials via ATRP. First, we carried out proof-of-concept grafting experiments by plasma deposition and coupling of macro-initiators to silicon wafers, gold quartz crystal microbalance (QCM) crystals, perfluorinated poly(ethylene-co-propylene) (FEP) film and multi-well microtitre plates. We then used SI-ATRP to graft polymer chains from these surfaces and characterized the materials to demonstrate that thick layers of polymer chains could be grown in the same fashion from inorganic and organic hard and soft materials. As potential biomaterial coatings, we wanted to show how the polymer brush system provides utility for different bulk materials. Our hypothesis was that these polymer brushes could used to reduce or eliminate protein adsorption to our grafted surfaces. Having identical coatings grafted from different substrates (soft polymeric samples and gold microsensors) allowed us to carry out parallel QCM and equilibrium binding studies. Our method allows brush biomaterials to be synthesized in a substrate-independent fashion according to our hypothesis and to identify system parameters allowing for improved resistance to protein adsorption. This research is important to biomaterial design and manufacture because our method eliminates substrate-specific linking chemistries and allows low-fouling polymer brush materials to be identically created from inorganic and organic hard and soft bulk materials following a single protocol.

2. Materials and methods

2.1. General

Square silicon wafer pieces were cut from 100 mm diameter wafer disks supplied by MMRC Pty Ltd. (VIC, Australia). Perfluorinated poly(ethylene-*co*-propylene) tape (Teflon FEP, 100 Type A) was supplied by DuPont (Riverstone, NSW, Australia). Gold-coated piezoelectric quartz crystals (QCM substrates) were obtained from Q-Sense (Q-Sense AB, Göteborg, Sweden). Tissue culture polystyrene (TCPS) plates (96-well, flat bottom) were purchased from BD (NSW, Australia). Allylamine (99%), α,α′-azoisobutyronitrile (AIBN, 98%), dichloromethane (DCM, >99.5%), 2-chloropropionyl chloride (97%), 2-hydroxyethyl methacrylate (97%), triethylamine (>99%), *N*,*N*′-dimethylacrylamide (DMA, 99%), 1, 1, 4, 7, 10, 10-hexamethylenetetramine (HMTETA, 97%), *N*-(3-dimethylaminopropyl)-*N*′-ethylcarbodiimide (EDC, ⩾97%), human serum albumin (HSA, 97–99%), lysozyme from chicken egg white, poly(ethylene glycol) methyl ether methacrylate with an average M_n of 475 g mol^{-1} (PEGMA475), sodium bisulfate and inhibitor-remover were obtained from Sigma–Aldrich. Ethylenediamine-tetraacetic acid disodium salt (EDTA, 99%) was obtained from BDH, Australia. Copper(II) chloride (⩾98%), sodium chloride and *N*,*N*-dimethylformamide (DMF, ⩾99.8%) were obtained from Merck Pty. Copper(I) chloride was purchased from Ajax Finechem, New Zealand. Dialysis membrane tubing (MWCO: 6–8000) was purchased from Sprectra/Por, USA. Acrylic acid (⩾99.0%) was purchased from Fluka. Reagents for the time-resolved fluorescence assay, such as DELFIA Europium labelling reagent, DELFIA enhancement solution and 100 nM Europium standard, were obtained from PerkinElmer, Australia. Opaque fluorescence reading plates were obtained from Grenier Bio-one, Germany. All water used was purified through a Milli-Q™ water purification system (Millipore Australia Pty) and had a resistivity of 18.2 MΩ cm. Phosphate-buffered saline (PBS, pH 7.2) solution was prepared from BupHTM packages (Thermo Scientific, USA) prepared in Milli-Q™ water. RBS-35® detergent concentrate was purchased from Thermo Scientific, USA.

2.2. Plasma polymerization

Initial surface functionalization was carried out using radiofrequency glow discharge (RFGD) techniques to deposit a cross-linked, organic thin film with amine functionality, using allylamine as a volatile "monomer". The radiofrequency field was generated in a custom-built reactor similar to the reported design [61]. The parameters chosen for the RFGD deposition of allylamine films were a frequency of 200 kHz and a load power of 20 W. The initial pressure of the reactor was 0.200 mbar and the treatment time was 25 s. For FEP film, plasma polymerization was carried out on both sides of the samples.

2.3. Initiator synthesis and coupling

A polymerizable ATRP initiator was prepared in the following manner. 2-Hydroxyethyl methacrylate (22.3 mmol) was stirred in a round bottom flask with 1.2 mol equivalent of triethylamine and approximately 15 ml of dichloromethane. 2-Chloropropionyl chloride (1.1 mol equiv.) was added drop-wise over the course of 1 h. After stirring overnight, the product was washed three times with 2% K_2CO_3 solution, passed through silica gel (1.09385.1000, Merck) and filtered, and the residual DCM was removed by rotary evaporation. The purity of the product, (2-(2-chloropropanoyloxy)ethyl methacrylate, 3.79 g) was confirmed by ^{1}H NMR and stored at −80 °C. The ^{1}H NMR shifts in DMSO-d_6, 400 MHz, were as follows: δ = 6.01 (s), 1H; δ = 5.68 (s), 1H; δ = 4.71 (q), 1H; δ = 4.37 (d), 2H; δ = 4.31 (d), 2H; δ = 3.22 (s), 3H; δ = 1.56 (d), 3H.

The poly-ATRP initiator (PATRPI) was synthesized in the following manner. Acrylic acid (1.5 g) was passed through a 6 ml column of inhibitor remover followed by 10 ml of DMF. A 0.52 g sample of 2-(2-chloropropanoyloxy)ethyl methacrylate and 0.0774 g of AIBN were added to the DMF/acrylic acid solution. This reaction was degassed at room temperature by purging with N_2 for 30 min. The copolymerization was initiated by heating to 70 °C and stirring

for 24 h. The resulting solution was dialysed against DMF for 3 days with daily solvent changes. The copolymer composition was analysed by ^{13}C NMR to determine the proportion of each monomer residue (^{13}C NMR (in DMF + $Cr(acac)_3$, 25 °C, 500 MHz) δ = 21.06, 39.51, 52.76, 60.11, 63.27, 169.60, 171.77, 175.88). By obtaining the ratio of the integrals of the carbonyl peaks at 171.77 (O=C–O), 169.60 (O=C–O, α Cl ester) and 175.88 (O=C–OH) ppm, the stoichiometry of the copolymer was found to be 88.7:11.3 mol.% acrylic acid:ATRP initiator.

Immediately after the allylamine RFGD thin film deposition, surfaces were placed in an initiator copolymer solution for coupling to the amine functionalized surface. PATRPI initiator copolymer solution was dissolved to 3 mg ml^{-1} in DMF and EDC was added (10 mg ml^{-1}) and mixed well. Substrates were immersed into the coupling solution (2 ml) and left to react overnight at room temperature under gentle agitation. To remove any non-covalently attached initiator, the surfaces were rinsed several times with DMF and water. When coupling to tissue culture polystyrene plates, the initiator was dissolved in DMF/water mixtures (7:2 by vol.) and 200 μl was added to each well.

2.4. Substrate preparation

Silicon wafer substrates were cut from the wafer into approximately 1 cm squares using a glass cutter. FEP was cut into small squares. The specific surface area of FEP was calibrated by preparing fifteen samples accurately cut into 1.00 cm squares and weighed. The surface area of FEP was calculated from its facial area. The mass per unit surface area (double-sided) was calibrated and gave a value of 0.0474 ± 0.002 mg mm^{-2}. Experimental surfaces were prepared by cutting the film to any size (typically squares of 1.27 cm) and then weighing. The stated thickness of FEP from the manufacturer is 50 μm. In calculations, we treated the thickness as making a negligible contribution to the surface area (an error estimated to be roughly 0.8% of the facial surface area).

Silicon wafers, gold-coated QCM sensors and FEP substrates were cleaned by sonicating in 2% RBS solution for 30 min, rinsing several times with water and ethanol, and drying using a purified nitrogen stream. Before use, substrates other than FEP were treated for 30 min by UV/Ozone treatment in a ProCleaner™ instrument from Bioforce Nanoscience, USA.

2.5. Synthesis of the grafted layers

The ATRP catalyst system was composed of activating and deactivating copper catalysts (Cu(I)Cl and $Cu(II)Cl_2$, respectively), with HMTETA as the chelating ligand. The molar proportions of monomer:CuCl:$CuCl_2$:HMTETA were 200:1:0.15:2. The reaction was scaled to 2 ml with water as the solvent. Monomer concentrations were varied in the range of 0.05–1.0 M.

Milli-Q™ water was degassed 10 times by evacuation on a high-vacuum line with nitrogen backfilling. Monomer was de-inhibited by stirring with inhibitor remover and bubbled with nitrogen for 30 min. The catalyst system was purged in a nitrogen atmosphere for 15 min before use. ATRP took place on a gently shaking platform in a nitrogen-filled glove box for 24 h at room temperature.

The reactions were quenched by exposing the solutions to air. The solution polymer was carefully extracted and saved for gel permeation chromatography (GPC) analysis. The substrates were washed with water, 50 mM Na_2EDTA, and 50 mM $NaHSO_3$ solutions. Finally, substrates were exhaustively washed with water and dried using a purified nitrogen stream. Complete removal of all traces of copper catalyst could be confirmed from the absence of copper peaks in X-photoelectron spectroscopy (XPS) survey spectra.

2.6. Polymer characterization

Solutions were collected post-polymerization and analysed by GPC for solution polymer. Samples were diluted in mobile phase (0.1 M sodium nitrate) and filtered through 0.2 μm filters before injection into a Shimadzu chromatography system (LC-20AD) pumping at 0.8 ml min^{-1}. The columns used were a 75 × 7.5 mm guard column (Bio-Rad), followed by Ultrahydrogel 2000 and 120 columns (300 × 7.8 mm, Waters Corporation), connected in series. Columns were maintained at 40 °C. The detectors used were a Dawn HELEOS II light scattering detector and an Optilab rEX refractive index detector (Wyatt Technology Corporation). Polydispersities were interpreted from ASTRA V software (Wyatt Technology Corporation) and molecular weight was calculated absolutely by using a value of 0.150 ml g^{-1} for the refractive index increment [50].

Peak areas were recorded for unpolymerized DMA appearing as a baseline-resolved, late-eluting peak in the chromatogram. This peak was distinguishable and separate from other low molecular weight species present in the solution polymer sample. In separate calibration experiments, known quantities of DMA were injected and used to plot a calibration curve of peak area versus concentration. The concentration of DMA remaining in samples post-polymerization was used to calculate monomer conversion.

2.7. X-ray photoelectron spectroscopy

XPS analysis was performed using an AXIS HSi spectrometer (Kratos Analytical Ltd., Manchester, UK), equipped with a monochromatic Al K_α source at a power of 144 W (12 mA, 12 kV). Charging of the samples during irradiation was reduced by an internal flood gun coupled with a magnetic immersion lens. Each sample was analysed at an emission angle normal to the sample surface. Survey spectra were acquired at 320 eV pass energy, and high-resolution C1*s* spectra were recorded at 40 eV pass energy. Data were processed with CasaXPS (ver. 2.3.13 Casa Software Ltd.), with residuals for curve fits minimized with multiple iterations using simplex algorithms. Spectra were corrected for charge compensation effects by offsetting the binding energy relative to the C1 (hydrocarbon) component of the C1*s* spectrum, which was set to 285.0 eV.

2.8. Quartz crystal microbalance with dissipation

The interaction of protein molecules with different surfaces was studied using the quartz crystal microbalance with dissipation (QCM-D) technique using an E4 instrument and software from Q-Sense, Sweden. Dynamic-equilibrium binding experiments were conducted in parallel using quartz crystal sensors modified with either (i) PATRPI or (ii) PATRPI grafted with poly-DMA (PDMA). The specimens were initially hydrated with PBS buffer until steady frequency (f) and dissipation (D) baselines were obtained under conditions of constant flow (0.1 ml min^{-1}) and temperature (20 °C). Protein solution (HSA, 0.1 mg ml^{-1} in PBS) was applied for 5 min followed by washing (Milli-Q™ water, 10 min, 1.0 M NaCl, 10 min) and re-equilibration in PBS. During washing, f traces were seen to deviate with large negative and positive deviations as the respective solutions interacted with the coated crystals. After re-equilibration, a stable, net negative frequency shift was interpreted as evidence of irreversible protein adsorption onto the substrate surface.

2.9. Europium-labelled HSA adsorption studies

Human serum albumin 1 mg (1.5×10^{-8} mol, Sigma, A3782, 99%, essentially fatty acid free) was added to 0.1 ml of a bicarbonate

buffer (pH 9.4) and an excess of Eu-labelling reagent (1.5×10^{-7} mol, Delfia Eu-N1 ITC chelate, Perkin Elmer). The reaction mixture was stirred and allowed to react at 4 °C overnight in the dark. The reaction was quenched by addition of Tris (tris(hydroxymethyl)methylamine) buffer. The Eu-HSA was purified from aggregated protein and excess labelling reagent using fast protein liquid chromatography (AKTA Purifier, GE Healthcare) equipped with a Superdex 75 size exclusion column (GE Healthcare, 30×1 cm) in Tris-buffered saline (pH 8). After purification, samples were taken for protein quantification using amino acid analysis (Water Alliance HPLC). This method of determining protein concentration has an accuracy of approximately 5%. The labelling ratio was determined by time-resolved fluorescence (PHERAstar multiwall plate reader, BMG Labtech; the excitation and emission wavelengths were 337 and 620 nm, respectively, with a count delay of 60 μs and count time of 400 μs) using the following procedure. An Eu calibration curve was determined by serial dilution of a 100 nM Eu standard (Perkin Elmer) in Delfia Enhancement solution (Perkin Elmer) and measurement of the time-resolved fluorescence counts as a function of Eu concentration (100 μl aliquots, five replicates). The purified Eu-HSA solution was also serially diluted with Delfia Enhancement solution and the time-resolved fluorescence counts determined (100 μl aliquots, five replicates). The number of moles of bound Eu was determined from comparison to the Eu calibration curve and found to be 4.2 mol Eu per mol HSA.

For static-equilibrium protein adsorption experiments, the fluorescence intensity of the stock Eu-HSA solution was attenuated by mixing the labelled protein with unlabelled HSA. Unlabelled HSA solution (1.00 mg ml^{-1}) and Eu-HSA (0.00668 mg ml^{-1}) were mixed in a 1:500 ratio (by protein mass) and finally diluted with PBS to a solution concentration of 0.1 mg ml^{-1}. FEP samples with various coatings were placed in an assay plate that had been freshly pre-blocked with 0.1 mg ml^{-1} HSA solution and exhaustively rinsed with PBS and Milli-Q™ water and dried. Substrate incubation commenced when prepared Eu-tagged protein solution was added (1 ml) and continued for 16 h under gentle shaking in the dark. Each sample condition was represented by three replicate FEP substrates. The untreated FEP control substrates were highly hydrophobic and remained unwetted at the air/liquid interface. After protein binding, substrates were washed five times with generous volumes of PBS. After the last wash, samples were carefully removed with tweezers and completely dried with purified nitrogen. Substrates were placed in 1.00 ml of enhancement solution and incubated in the dark for 45 min. Aliquots of Eu-complex solution (4×0.1 ml) were transferred to an opaque microtitre plate and read using the time-resolved fluorescence assay on the PHERAstar instrument. Protein adsorption results were expressed as the average protein amount bound (ng cm^{-2}), with uncertainties representing variance in the three replicate samples. This method of measuring protein adsorption is very similar in many respect to methods using radiolabelled proteins (e.g. via ^{125}I), except that an Eu-chelated label is chemically coupled to the protein molecules instead of a radiolabel. A similar sensitivity is obtained with both methods (i.e. the sensitivity of the Eu assay is on the order of femtomoles of Eu-labelled protein).

3. Results

3.1. Choice of substrate

The surface modification procedure was applied to a diverse array of flat materials: inorganic and organic; rigid and flexible. Silicon wafers were chosen for proof-of-concept grafting experiments. Gold-coated quartz crystals were chosen for their applicability for QCM experiments. FEP film and TCPS microtitre plates were used to provide examples for grafting from polymeric substrates. FEP is transparent and easily cut, and can be functionalized on both sides to provide a uniform, relatively high-surface-area substrate with macroscopic dimensions. To illustrate that hard polymeric substrates of complex geometries could be modified, 96-well microtitre plates were used.

3.2. Aqueous ATRP grafting of PDMA from flat surfaces

A polymerizable ATRP initiator (compound **1**) was synthesized according to Fig. 1. This was then copolymerized to form an acrylic-acid-based random copolymer macro-initiator containing ATRP residues called poly-ATRP initiator (PATRPI). The composition of acrylic acid to ATRP initiator moieties in the copolymer was determined to be 0.887:0.113 by ^{13}C NMR.

Initiator functionalization of any of the surfaces proceeded as depicted in Fig. 2. Presented in Table 1 are the elemental atomic concentrations from XPS survey scans for FEP initiator modification. When the allylamine plasma polymer (ALAPP) plasma coating was applied, there was a large reduction in fluorine and a noticeable increase in the nitrogen content (Table 1). After coupling with PATRPI, the C6 component (Fig. 3), assigned to fluorocarbon photoelectrons (C–F), was observed to diminish to baseline values. Also, the amount of fluorine in the plasma-functionalized sample surface (6.9%) decreased to below the detectable level for the instrument in the PATRPI sample. Elimination of the fluorine signal suggested that the initiator copolymer layer and the ALAPP thin film together formed a thick coating on FEP exceeding the XPS sampling depth (approximately 10 nm). Further evidence for incorporation of ATRP initiators was shown by the presence of a weak elemental signal from the presence of chlorine (0.126%) on the PATRPI surface.

The PATRPI overlayer partially attenuated the underlying nitrogen XPS signal. Based on the value for the inelastic mean free path for ejected F1*s* or N1*s* photoelectrons travelling through a polymer layer [62], we estimated the layer thickness based on a previously described method [63]. We averaged the XPS results from many of our surfaces prepared under similar experimental conditions and determined the thickness of the PATRPI layer to be 0.54 ± 0.18 nm. Knowing the composition of the initiator and assuming a similar density to poly(acrylic acid) (1.5 g cm^{-3}), we estimated the number of ATRP initiator residues present to be 0.62 ± 0.20 initiators per square nanometre.

After SI-ATRP using different concentrations of DMA, evidence for increasing amounts of surface-grafted PDMA was observed, as shown in Fig. 4. In contrast to the sample where [DMA] = 0.05 M, which appeared almost indistinguishable from the initiator-functionalized surface, for [DMA] = 0.15 M and 0.50 M, the high-resolution C1*s* component corresponding to C4 (C–N, amide) increased prominently. Furthermore, the C5 component (O═C–O, acid) associated with the initiator copolymer layer decreased dramatically in intensity.

The data presented in Fig. 5 illustrates that very similar high-resolution C1*s* XPS spectra were obtained for PDMA layers grafted from three different substrates. Silicon wafers, FEP film and TCPS well bottoms are compared to show that near-identical polymer coatings were polymerized from different substrates using the same reaction scheme followed by SI-ATRP using [DMA] = 0.5 M. The peaks obtained were characteristic of PDMA layers which had a thickness equivalent to or greater than the XPS sampling depth of approximately 10 nm (see Fig. 4). For bulk PDMA, we would expect the fractional peak area of the amide (C4) over the total carbon to be 0.20. In Fig. 5, the C4 components show better than 95% agreement with this target (the percentages of C4/C were 0.19 for silicon, 0.19 for FEP and 0.20 for the 96-well plate bottoms).

We also studied thick PDMA layers produced by grafting with [DMA] = 2.0 M as a platform for investigating the "livingness" of

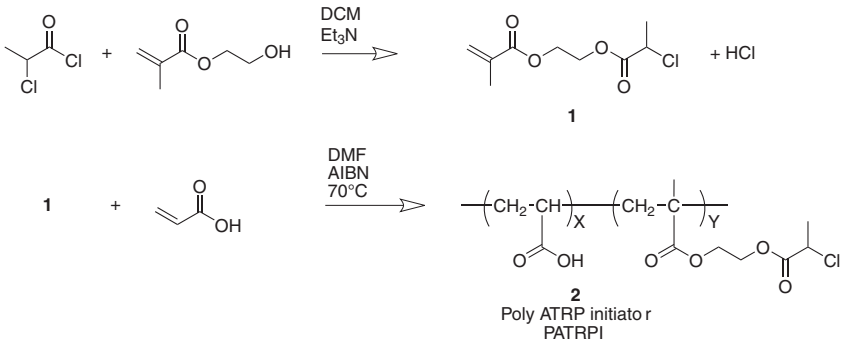

Fig. 1. Schematic illustration for the synthesis of PATRPI.

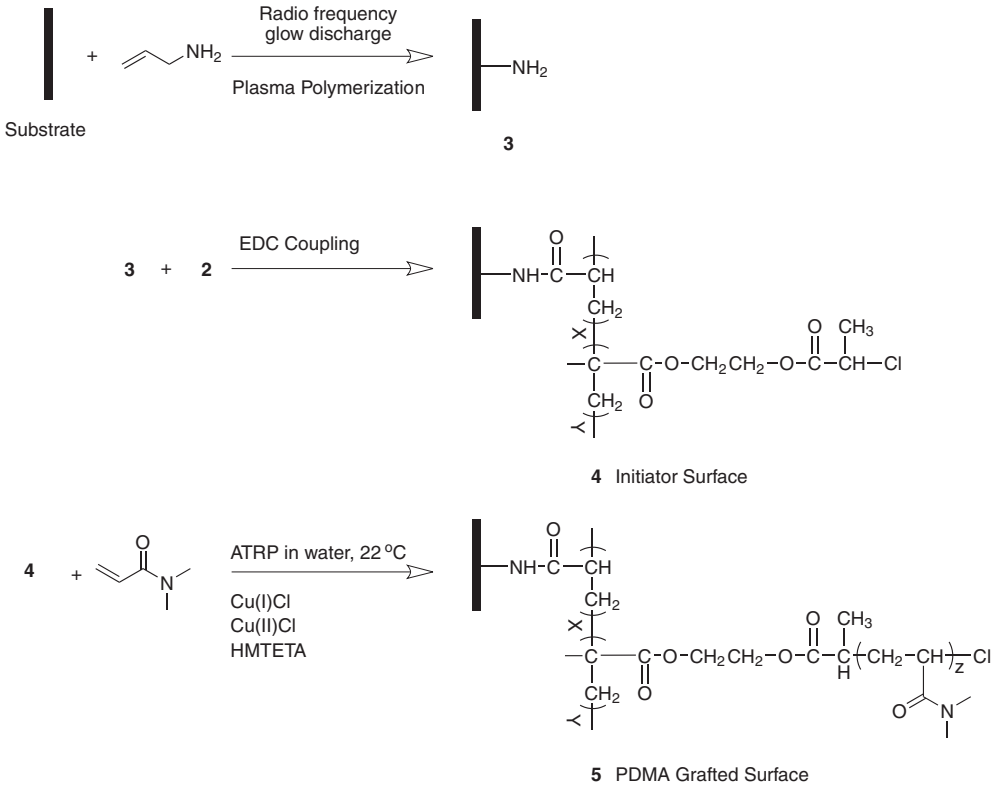

Fig. 2. Modification schematic for initiator functionalization and polymer grafting.

Table 1
XPS elemental analysis for FEP tape coated with polymer layers.

		Atomic concentration (%)				
		F	O	N	C	Cl
Substrate control	Uncoated FEP	63.3	–	–	37.6	–
Plasma control	Allylamine plasma polymer	6.87	12.6	10.8	69.8	–
Initiator control	PATRPI	–	11.3	10.9	75.6	0.126
Grafted samples	[DMA] = 0.05 M	–	13.8	10.6	75.6	–
	[DMA] = 0.15 M	–	13.7	11.7	74.6	–
	[DMA] = 0.50 M	–	13.3	12.7	74.0	–

the reaction. After washing and drying, PDMA-grafted silicon wafers were placed in a new vessel with fresh catalyst, solvent and polyethylene glycol ($M_w \sim 475$) methacrylate (PEGMA475). The high-resolution C1*s* XPS spectrum for the grafted PDMA-block-PEGMA layers (Fig. 6) were indicative of a thick layer of PEGMA, rich in C3 component (ether) and nearly complete attenuation of the C4 (amide) from the underlying PDMA block (Fig. 6).

Properties of the surface polymer could be inferred from GPC analysis of the bulk solution collected above the polymerized surface post-reaction (Table 2). From the residual monomer quantified, the [DMA] = 0.05 M sample had a very low conversion, which was below the 1.5% variance observed from replicate analysis of four samples. Up to 36% conversion was observed for the [DMA] = 0.50 M sample.

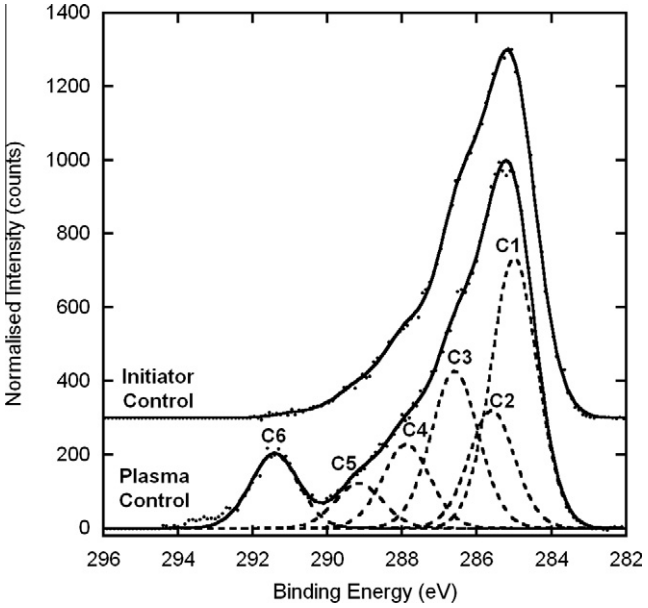

Fig. 3. High-resolution XPS scan of the C1*s* region of FEP substrates functionalized with allylamine plasma polymer (plasma control) or PATRPI copolymer (initiator control). Curve fits to the data comprising six components (dashed lines) are shown for the plasma control as an example.

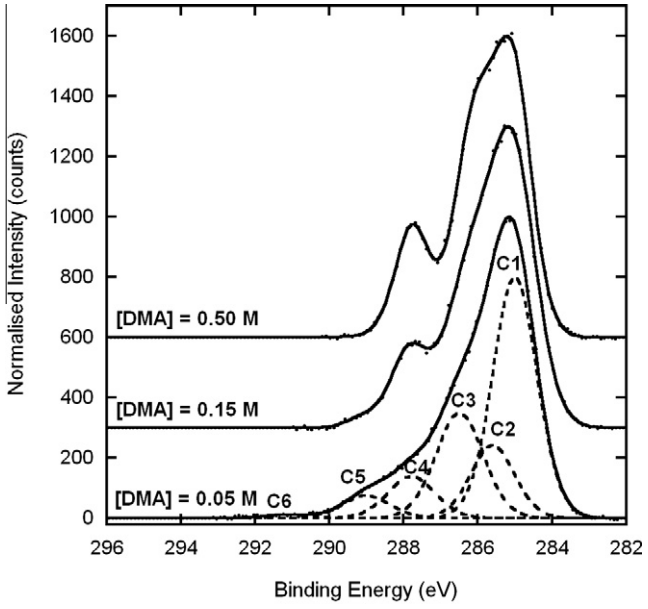

Fig. 4. High-resolution XPS scan of the C1*s* region of FEP substrates with different monomer concentrations. Curve fits to the data comprising six components (dashed lines) are shown for the [DMA] = 0.05 M graft layer as an example.

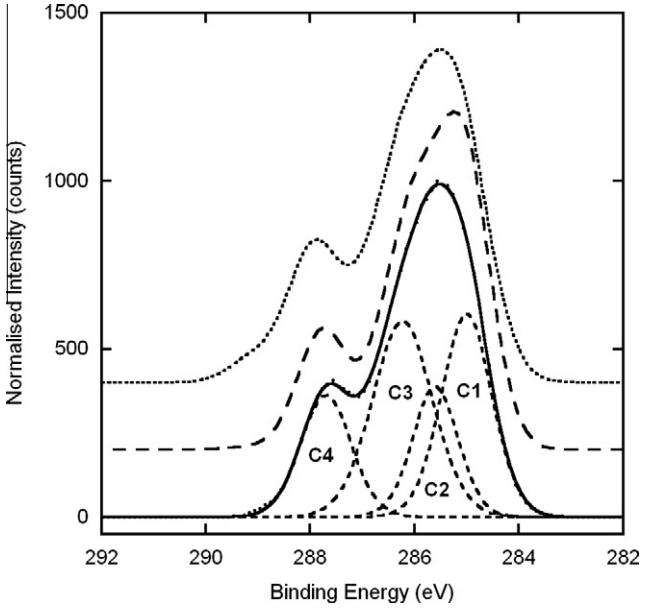

Fig. 5. High-resolution XPS scan of the C1*s* region of PDMA grafted from TCPS (top), FEP (middle) and Si wafer (bottom).

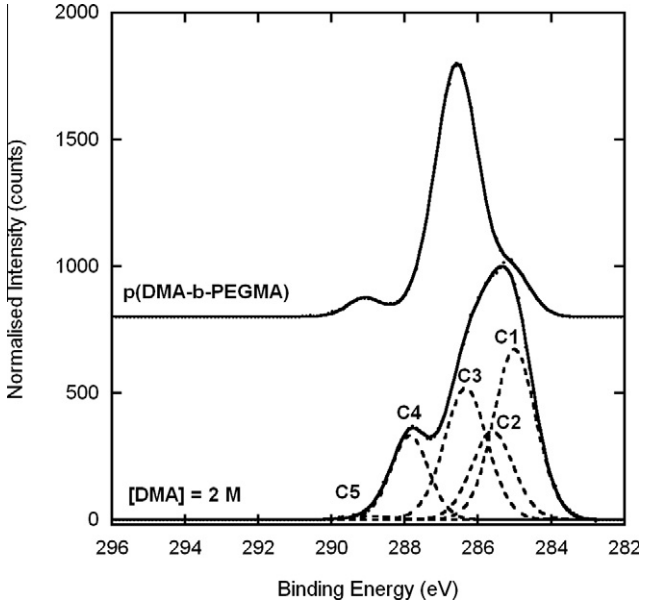

Fig. 6. High-resolution XPS scan of the C1*s* region of a silicon wafer grafted with [DMA] = 2 M (lower curve). When this surface was washed, dried and then introduced to a new solution containing fresh solvent, catalyst and [PEGMA475] = 1 M, a block copolymer was produced with a spectrum (upper curve) which was characteristic of PEGMA475 polymer. Curve fits to the data comprising six components (dashed lines) are shown for the [DMA] = 2 M grafted sample as an example.

The solution polymer molecular weight increased with the DMA feed concentration. A maximum molecular weight of 303 kDa was observed for the [DMA] = 0.50 M sample, mirroring the very thick grafted layer observed for the surface-grafted counterpart.

3.3. QCM-D studies

The same reaction procedure shown in Fig. 2 was applied to gold-coated QCM substrates. HSA adsorption onto PDMA-grafted surfaces prepared using SI-ATRP was compared to that obtained with the initiator control (PATRPI) surface to investigate whether the presence of the grafted layer would reduce protein adsorption under dynamic-equilibrium binding (flow) conditions. Fig. 7 shows the decreased frequency shifts obtained when a 0.1 mg ml^{-1} HSA solution was applied to the PATRPI surface (i.e. initiator only). Negative shifts in frequency were diagnostic of increased mass coupled to the crystal (i.e. protein has adsorbed to the surface). The *f* shift of −14 Hz observed persisted after extensive washing in buffer, salt solution and water. We did not attempt to correlate the observed frequency shift to a mass increase because of the difficulty in applying a meaningful viscoelastic model to the multi-layered polymer architecture. No such frequency shift was observed with

Table 2
Solution polymer properties from polymerization reactions on modified FEP determined by GPC.

[DMA] in feed (M)	DMA conversion[a] (%)	Solution PDMA M_n (kDa)	Solution PDMA M_w/M_n
0.05	<1.5	38	1.2
0.15	17.0 ± 3.2	96	1.1
0.50	36.2 ± 1.5	303	1.3

[a] Uncertainties are based upon standard error in determining values from four samples under identical graft conditions (95% confidence).

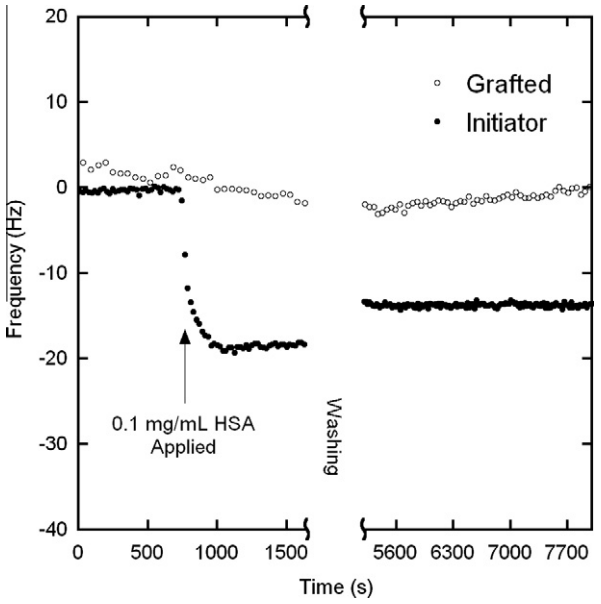

Fig. 7. QCM-D experiment demonstrating the effect of applying 0.1 mg ml^{-1} HSA (indicated by the arrow) to substrates functionalized with either initiator or PDMA grafted polymer ([DMA] = 0.5 M). Washing involved at least 5 min applications of buffer, 1 M NaCl and water, followed by re-equilibration in buffer. Frequency shifts to lower values correlate with an increase in mass coupled to the surface.

the 0.5 M DMA-grafted surface, indicating that no protein adsorbed to the surface within experimental error. We repeated this experiment using higher concentrations of HSA (1.0 mg ml^{-1}) and lysozyme (1.0 mg ml^{-1}), but did not observe any meaningful f shifts indicating protein adsorption to the surface.

3.4. Europium-labelled protein adsorption

Protein adsorption to PDMA-grafted FEP films was quantified using a time-resolved fluorescence assay with Eu-tagged HSA incubated overnight in a static-equilibrium binding experiment. Fig. 8 shows the amount of bound HSA in response to different concentrations of DMA used in the ATRP reaction. All modified surfaces had reduced protein adsorption when compared to unmodified FEP, with the three PDMA grafted surfaces showing a significant reduction (one-tailed t-test assuming unequal variance, 95% confidence).

4. Discussion

We have developed a new technique for applying a general SI-ATRP procedure to inorganic/metal and organic substrates; both rigid and flexible. As exemplified on different classes of bulk materials (a semi-conductor, a metal, molded plastic laboratory microtitre plates and a flexible polymer film), a key feature of this

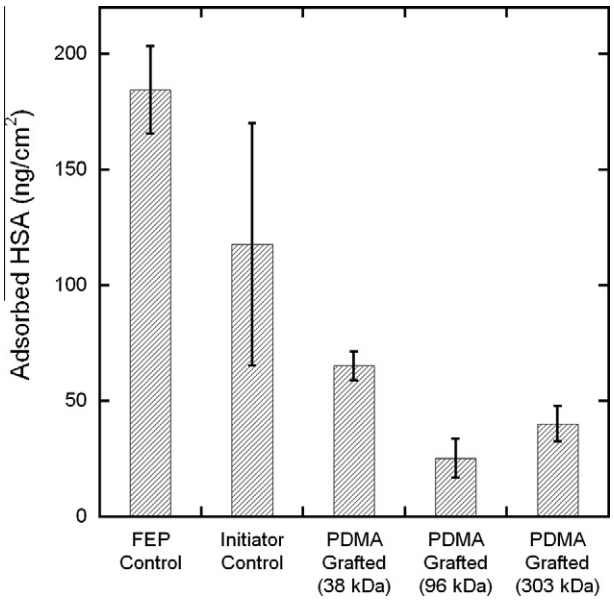

Fig. 8. Eu-tagged HSA adsorbed onto experimental FEP surfaces. Surfaces were incubated with 0.1 mg ml^{-1} Eu-HSA in PBS for 18 h, then exhaustively washed and blown dry with nitrogen. Enhancement solution was incubated with the surfaces allowing for dissociation of the europium tag. Aliquots were quantified in a time-resolved fluorescence assay.

procedure is the potential applicability to graft from any type of flat substrate. Plasma polymer deposition followed by coupling of an ATRP macro-initiator allowed for terminally attached polymer chains to be grown from these materials through covalently attached interlayers.

4.1. Surface-Initiated ATRP

In this study we have verified that each of our test surfaces could be functionalized with an ATRP macro-initiator and act as a platform for performing SI-ATRP. Covalent linking of the macro-initiator to any of the substrates is made possible by substrate treatment with a plasma polymer interlayer derived from allylamine. Plasma polymerization is a complex process involving the monomer, and radicals and ions derived from excitation in the plasma phase [64]. At the surface, rearrangement and polymerization of the monomer forms network linkages to the substrate. Although the nature of the substrate plays a role in very thin plasma polymer layers, by the time film growth has reached many nanometres, as is the case here (approximately 10–20 nm), the physical properties of the polymer layer are essentially the same regardless of the underlying substrate [65]. The broad use of plasma polymerization for forming covalent interlayers in, for example, biomolecule immobilization has been shown to be a versatile and emerging platform technology [66]. XPS survey data support the grafting paradigm (Fig. 2) where expected changes in the surface elemental compositions can be interpreted logically from diagnostic elements present or absent in the successive overlayers (Table 1). High-resolution C1s spectra also show the presence of the initiator layer covering the base substrate with, for example, nearly complete attenuation of the C6 (C–F) component when the macro-initiator was coupled to FEP (Fig. 3). That successively thicker PDMA layers could be grafted in response to increasing [DMA] is shown qualitatively in Fig. 4. Evidence for increased thickness can also be inferred semi-quantitatively from the increasing N/C ratio relative to the theoretical value of 0.200 for the pure polymer. From Table 1, N/C was calculated to be 0.140, 0.157 and 0.172 for [DMA] = 0.05, 0.15 and 0.5 M, respectively.

Post-polymerization, these solutions were found to contain low-polydispersity PDMA chains (Table 2), even though no sacrificial initiator was used in the monomer solution. This observation was not unexpected, based on past experience [50]. The solution polymer has previously been shown to be a very good predictor of the properties of immobilized polymer chains when cleaved from the substrate and analysed under similar conditions (i.e. here we have used the same monomer, transition metal catalyst system, ligand, solvent, temperature, reaction duration and ATRP initiator residue) [50]. In this study we were not able to recover detectable amounts of cleaved surface polymer because of the very low surface areas used. Table 2 shows an increasing trend in polymer molecular weight with increasing monomer concentration and polydispersities in solution polymer from grafted FEP film, indicating that the reaction was controlled. We expect these trends to be mirrored on the surface as long as there is sufficient mass transfer ensuring good mixing between the surface and solution phases. Additionally, the "livingness" of the SI-ATRP reaction was demonstrated (Fig. 6) by creating grafted materials with PDMA whose chain ends could then be reinitiated to make poly(PEGMA475) block copolymers. The assumed congruence between the solution and surface polymer properties, together with supporting evidence from XPS surface characterization and the demonstration of chain "livingness", completes the picture that low-polydispersity PDMA chains were successfully grafted by SI-ATRP from our substrates.

The versatility of this technique is best shown by Fig. 5, where identical PDMA layers were shown to be grafted from a diverse array of material substrates. High-resolution C1*s* XPS spectra reveal nearly identical (full thickness) PDMA coatings grafted from TCPS, FEP and silicon. This suggests that our coating methodology allows for substrate-independent SI-ATRP to be achieved. Next we built on this work by expanding the range of substrates and observing the biological response to discuss the potential role of these grafted surfaces as low-fouling surfaces.

4.2. Protein adsorption studies

New fabrication strategies are used to produce novel coatings for biomedical devices in an attempt to mediate the biological response at the surface interface. Since protein adsorption occurs rapidly to surfaces the moment they are exposed to biological fluids [67], a common first step in the development of new coatings is to evaluate protein adsorption. Surfaces grafted with terminally attached polymer chains are known to reduce or eliminate protein adsorption to surfaces (at least to the detection limit of the various techniques used) based on the principle of entropic exclusion. Exclusion of proteins from the surface interface has commonly been evaluated using model protein probes, which provide a demonstration of their low-fouling ability [3,4]. Even though limited protein binding experiments may or may not comprehensively account for aspects of real-world protein fouling (such as the effects of having very large or very small proteins, their affinities for the surface, variations in their isoelectric points), the use of model proteins in binding studies is instructive in validating the exclusion principle in a specific grafting experiment. It is the broad customizability of the SI-ATRP grafting technique and initiator immobilization strategies (where the monomer, graft length and graft density can be varied, and also the novel macro-initiator surface modification method presented here) that will provide greater applicability in the fabrication of real-world biomedical device coatings as the research field continues to broaden.

Stretching of grafted chains away from a surface is a function of the grafted polymer's molecular weight, the grafting density and the nature of the polymer itself in a given solvent [68]. Studies at constant molecular weight and increasing graft density show that as the chain arrangements become more densely packed, the system gains more of an entropic driving force to facilitate improved protein rejection [36]. Similarly, since chains occupy more space as their molecular weight is increased (self-avoidance), grafting longer chains from a constant density surface will promote more near-neighbor collisions also giving rise to more chain stretching in the system. It is this second approach that we have applied in our study. Our goal was to demonstrate the principle of entropic exclusion of model proteins from grafted layers using our new initiator and immobilization method to evaluate what we define as their "low-fouling" ability. Evaluation has been carried out using two different experimental protocols. With the QCM-D technique, protein adsorption to grafted surfaces was evaluated under flow conditions. This experimental design considers that chain morphology may be disturbed under the influence of flow and that the surface is being constantly exposed to fresh protein solution. This dynamic-equilibrium study contrasts the classical soak-and-rinse protein binding experiment discussed later, which ensures that the system has come to static-equilibrium.

Fig. 7 shows that, in a QCM-D experiment, initiator control samples exposed to 0.1 mg ml^{-1} HSA solution resulted in a significant negative change in frequency of the QCM sensor. After extensive washing, a permanent deflection was noted, indicating irreversible adsorption. PDMA-grafted samples showed no mass increase after washing showing that protein was prevented from adsorbing to the surface or underling initiator layer by the end grafted polymer layer. This effect did not appear to be a consequence of the protein concentration or type. The result was the same for HSA at a higher concentration of 1.0 mg ml^{-1} as well as for smaller-molecular-weight proteins with higher isoelectric points (lysozyme), even at high concentrations of 1.0 mg ml^{-1} (data not shown). To conclude, we did not observe any lysozyme or HSA adsorption to grafted QCM crystals in dynamic-equilibrium binding assays.

We also conducted static-equilibrium protein adsorption experiments using labelled HSA in order to quantify protein adsorption onto surfaces grafted with polymers of different molecular weights. Surfaces were exposed to a solution of protein and left to equilibrate over 16 h, then evaluated. Contrasting the flow conditions used above, we would expect that under static-equilibrium binding conditions, grafted chains would adopt the most energetically favourable conformations in the absence of flow. Here FEP was used since it is easily handled and simply cut to a defined surface area.

We observed that all surfaces with the exception of unfunctionalized FEP were readily wetted by water. The hydrophobic nature of bare FEP clearly promoted a large amount of protein adsorption to the surface (Fig. 8). As a general point of comparison for HSA adsorption to naked surfaces, others have shown that the maximum (monolayer) coverage varies between 100 and 300 ng cm^{-2}, depending on variations in the experimental conditions [69]. Our results for naked FEP are in this range (184 ng cm^{-2}), with the experimental error principally associated with a difficulty in exposing this highly hydrophobic surface to the test solution. We have included this sample and the initiator control sample (118 ng cm^{-2}) to demonstrate that the initiator modification (and subsequent grafting) rendered the film completely hydrophilic, as well as to give a baseline value for comparison with grafted surfaces.

For grafted surfaces, we have assumed that SI-ATRP using solutions of different DMA concentrations resulted in surface coatings with constant graft density. Indeed, others who have studied similar systems (aqueous SI-ATRP of DMA) demonstrate that, for [DMA] lower than 0.5 M, changes in [DMA] have little influence on graft density [22]. Assuming the characteristics of solution polymer are representative of the surface polymer (which we know from other experimental work on similarly sized flat surfaces using a similar initiating system), we feel confident that the effects seen

in Fig. 8 are predominantly due to changes in the chain molecular weight at constant graft density.

It appears that PDMA chains of low molecular weight (38 kDa) have sufficient entropy to prevent a great deal of protein adsorption on FEP substrates, reducing the amount of bound protein by 45% compared to the initiator surface and 65% compared to naked FEP (Fig. 8). A further reduction in adsorbed protein (79% reduction relative to the initiator and 86% relative to FEP) was observed for the sample with the second highest PDMA chain molecular weight (polymer = 96 kDa). This was the minimum level observed in this study (25 ng cm^{-2}). For surfaces grafted with longer PDMA chains, we observed a slight increase (but not significantly different) in the amount of protein adsorbed to the surface (two-tailed *t*-test with unequal variance, 95% confidence). Assuming constant graft density, and knowing that the highly stretched polymer brush conformation is crucial to the reduction of protein adsorption [70], we can conclude that, for lower-molecular-weight graft layers, the polymer chain conformation is less stretched (or possibly in the mushroom regime) and will have a diminished ability to prevent surface fouling. The use of longer chains (96 kDa and larger in this study) suggests that increased chain stretching is present in the system, allowing a larger effect from entropy-driven exclusion – to a point. Beyond 96 kDa, analysis of the data suggests that we must consider that the longer chains have an increased number of chain-protein contacts. This could provide an enthalpic driving force, resulting in increased protein adsorption, as observed by others [71].

We can compare our protein adsorption studies with that of the Lai and colleagues from the Kizhakkedathu group [36]. Although we used different assay and detection methods, the fact that Lai et al. completed the most comprehensive study of protein adsorption to PDMA-grafted surfaces allows for a more relevant and insightful comparison to be drawn to this work than any other published work.

In the work of Lai et al., experiments involving blood plasma protein adsorption to PDMA surfaces provide relevance for biomedical device fabrication by showing how grafted surfaces interact with a complex protein mixture with the aim of creating antithrombotic surfaces. Here, surfaces were prepared with increasing graft density and a constant graft molecular weight (approximately 30.4 kDa). At high graft densities, there was an approximately 85% reduction in plasma protein adsorption to PDMA grafted surfaces. In our system, at certainly lower graft density, we achieved a similar reduction in protein adsorption (86% compared to unmodified FEP and using HSA), but only when the molecular weight of our chain was higher than 96 kDa. For the sake of comparison, our low molecular weight chains (38 kDa) were effective at reducing HSA adsorption by 65% compared to ungrafted FEP. If we compare the results for PDMA chains on the order of 30–40 kDa, we can see that the greater density in Lai et al. allows for a larger protein-exclusion effect to manifest even with smaller chains due to the entropy present in the system. We are able to compensate in our system at lower graft density by grafting larger molecular weight chains. Although we should be cautious about over-generalizing our results from what may be perceived as inaccurate comparisons (i.e. comparing HSA in our study to adsorption of all blood plasma proteins in the other and at different concentrations), one point that we can confidently reiterate is that PDMA chains grafted by either SI-ATRP technique allows for significant reduction in protein adsorption, far below monolayer coverage, based on the principles of entropic repulsion by terminally grafted chains.

We have used these protein adsorption studies only as a demonstration of this principle, as the fabrication method was the focus of our work. However, others have instructively shown the way to exploit this principle, further reducing or completely eliminating measurable protein adsorption on grafted surfaces by, for example, increasing the graft density or forming different polymer chains [31,36,72,73]. We have already shown the use of two monomers in our work, but substitution of other "biocompatible" monomers commonly used in ATRP could be easily demonstrated. We also suggest that it would be easy to manipulate the graft density since our macro-initiator can be customized to include variable proportions of ATRP initiators. Both of these approaches encompass efforts that were beyond the scope of this paper and are the subject of a forthcoming publication. We conclude by discussing an insight into protein adsorption studies made possible by the use of our substrate-independent approach.

We observed a difference in protein adsorption to similarly grafted samples using [DMA] = 0.5 M that was dependent on whether measured under soaking conditions or under flow conditions in a QCM flow cell. Differences in chain morphology under the influence of flow is a likely reason why we observed zero protein adsorption in the QCM-D flow cell (dynamic-equilibrium) experiments but a small amount of protein adsorption in experiments conducted under static-equilibrium conditions. This difference in results can be understood in the context of a previous study, where we observed that the partition coefficient for a model protein (bovine serum albumin) into a PDMA brush decreased with increasing flow rate – likely due to stretching and tilting of the grafted polymer under the influence of shear flow [49]. These experiments importantly illustrate that, during experimentation, disturbing the chain conformation under the influence of flow potentially alters evaluation of the protein-fouling characteristics of identically grafted polymer brushes from what could be considered "anti-fouling" with our QCM results to "low-fouling" from our static-equilibrium protein adsorption results.

5. Conclusions

This paper described a general scheme for covalent surface modification of flat substrates with terminally grafted polymers. Use of plasma modification in the first step removed substrate-dependent linking chemistries and has allowed us to demonstrate successful graft modification of soft and hard organic and inorganic substrates.

We were able to generate PDMA graft layers using SI-ATRP from silicon wafers, QCM crystals, TCPS microtitre plates and FEP film using a grafting method based on a surface-attached initiator. Despite being very different bulk materials, the surfaces of each could be treated in the same way to achieve the same coating. This finding is highly applicable to the design of new biomaterials, providing a platform strategy in which different bulk materials provide the form and the coating provides the function. One application of this technology to biosciences was exemplified by demonstrating that coatings were able to render surfaces resistant to non-specific protein adsorption. Dynamic-equilibrium protein binding experiments showed that PDMA-grafted chains were able to completely prevent protein adsorption to the grafted QCM crystal. Static-equilibrium protein binding assays showed decreased protein adsorption as a function of surface graft polymer molecular weight, suggesting that, given that the graft density was constant in this study, increasing the molecular weight of the grafted chains moved the polymer chains from a less stretched (or possibly a mushroom conformation) towards a more highly stretched polymer brush conformation.

Acknowledgements

We acknowledge the efforts of The International Association for the Exchange of Students for Technical Experience (Y.L.) and the Cooperative Research Centre for Polymers for funding (B.R.C.).

We are grateful to Mr. John Bentley for assistance in europium labelling of HSA, and Dr. Jo Cosgriff and Dr. Roger Mulder for assistance with NMR.

References

[1] Pyun J, Kowalewski T, Matyjaszewski K. Synthesis of polymer brushes using atom transfer radical polymerization. Macromol Rapid Commun 2003;24:1043–59.

[2] Tsujii Y, Ohno K, Yamamoto S, Goto A, Fukuda T. Structure and properties of high-density polymer brushes prepared by surface-initiated living radical polymerization. In: Jordan R, editor. Surface-Initiated Polymerization I. Berlin: Springer-Verlag; 2006. p. 1–45.

[3] Fristrup CJ, Jankova K, Hvilsted S. Surface-initiated atom transfer radical polymerization – a technique to develop biofunctional coatings. Soft Matter 2009;5:4623–34.

[4] Barbey R, Lavanant L, Paripovic D, Schüwer N, Sugnaux C, Tugulu S, et al. Polymer brushes via surface-initiated controlled radical polymerization: synthesis, characterization, properties, and applications. Chem Rev 2009;109:5437–527.

[5] Coessens V, Pintauer T, Matyjaszewski K. Functional polymers by atom transfer radical polymerization. Prog Polym Sci 2001;26:337–77.

[6] Edmondson S, Osborne VL, Huck WTS. Polymer brushes via surface-initiated polymerizations. Chem Soc Rev 2004;33:14–22.

[7] Husseman M, Malmstrom EE, McNamara M, Mate M, Mecerreyes D, Benoit DG, et al. Controlled synthesis of polymer brushes by "living" free radical polymerization techniques. Macromolecules 1999;32:1424–31.

[8] Zhao B, Brittain WJ. Synthesis, characterization, and properties of tethered polystyrene-b-polyacrylate brushes on flat silicate substrates. Macromolecules 2000;33:8813–20.

[9] Piech M, Bell NS. Controlled synthesis of photochromic polymer brushes by atom transfer radical polymerization. Macromolecules 2006;39:915–22.

[10] Zhai G, Cao Y, Gao J. Covalently tethered comb-like polymer brushes on hydrogen-terminated Si (100) surface via consecutive aqueous atom transfer radical polymerization of methacrylates. J Appl Polym Sci 2006;102:2590–9.

[11] Edmondson S, Huck WTS. Controlled growth and subsequent chemical modification of poly(glycidyl methacrylate) brushes on silicon wafers. J Mater Chem 2004;14:730–4.

[12] Xu D, Yu WH, Kang ET, Neoh KG. Functionalization of hydrogen-terminated silicon via surface-initiated atom-transfer radical polymerization and derivatization of the polymer brushes. J Colloid Interface Sci 2004;279:78–87.

[13] Ayres N, Boyes SG, Brittain WJ. Stimuli-responsive polyelectrolyte polymer brushes prepared via atom-transfer radical polymerization. Langmuir 2007;23:182–9.

[14] Kim JB, Bruening ML, Baker GL. Surface-initiated atom transfer radical polymerization on gold at ambient temperature. J Am Chem Soc 2000;122:7616–7617.

[15] Ejaz M, Tsujii Y, Fukuda T. Controlled grafting of a well-defined polymer on a porous glass filter by surface-initiated atom transfer radical polymerization. Polymer 2001;42:6811–5.

[16] Gao X, Feng W, Zhu S, Sheardown H, Brash JL. A facile method of forming nanoscale patterns on poly(ethylene glycol)-based surfaces by self-assembly of randomly grafted block copolymer brushes. Langmuir 2008;24:8303–8.

[17] Feng W, Chen RX, Brash JL, Zhu SP. Surface-initiated atom transfer radical polymerization of oligo(ethylene glycol) methacrylate: effect of solvent on graft density. Macromol Rapid Commun 2005;26:1383–8.

[18] Ignatova M, Voccia S, Gilbert B, Markova N, Cossement D, Gouttebaron R, et al. Combination of electrografting and atom-transfer radical polymerization for making the stainless steel surface antibacterial and protein antiadhesive. Langmuir 2006;22:255–62.

[19] Lego B, Skene WG, Giasson S. Unprecedented covalently attached ATRP initiator onto OH-functionalized mica surfaces. Langmuir 2008;24:379–82.

[20] Xiao DQ, Zhang H, Wirth M. Chemical modification of the surface of poly(dimethylsiloxane) by atom-transfer radical polymerization of acrylamide. Langmuir 2002;18:9971.

[21] Desai SM, Solanky SS, Mandale AB, Rathore K, Singh RP. Controlled grafting of N-isopropyl acrylamide brushes onto self-standing isotactic polypropylene thin films: surface initiated atom transfer radical polymerization. Polymer 2003;44:7645–9.

[22] Zou Y, Kizhakkedathu JN, Brooks DE. Surface modification of polyvinyl chloride sheets via growth of hydrophilic polymer brushes. Macromolecules 2009;42:3258–68.

[23] Ohno K, Kayama Y, Ladmiral V, Fukuda T, Tsujii Y. A versatile method of initiator fixation for surface-initiated living radical polymerization on polymeric substrates. Macromolecules 2010;43:5569–74.

[24] Xu FJ, Zhong SP, Yung LYL, Kang ET, Neoh KG. Surface-active and stimuli-responsive polymer-si(100) hybrids from surface-initiated atom transfer radical polymerization for control of cell adhesion. Biomacromolecules 2004;5:2392–403.

[25] Feng W, Zhu SP, Ishihara K, Brash JL. Adsorption of fibrinogen and lysozyme on silicon grafted with poly(2-methacryloyloxyethyl phosphorylcholine) via surface-initiated atom transfer radical polymerization. Langmuir 2005;21:5980–7.

[26] Dong R, Krishnan S, Baird BA, Lindau M, Ober CK. Patterned biofunctional poly(acrylic acid) brushes on silicon surfaces. Biomacromolecules 2007;8:3082–92.

[27] Lee BS, Chi YS, Lee KB, Kim YG, Choi IS. Functionalization of poly(oligo(ethylene glycol)methacrylate) films on gold and Si/SiO_2 for immobilization of proteins and cells: SPR and QCM studies. Biomacromolecules 2007;8:3922–9.

[28] Tugulu S, Klok HA. Stability and nonfouling properties of poly(poly (ethylene glycol) methacrylate) brushes under cell culture conditions. Biomacromolecules 2008;9:906–12.

[29] Bernards MT, Cheng G, Zhang Z, Chen S, Jiang S. Nonfouling polymer brushes via surface-initiated, two-component atom transfer radical polymerization. Macromolecules 2008;41:4216–9.

[30] Stadler V, Kirmse R, Beyer M, Breitling F, Ludwig T, Bischoff FR. PEGMA/MMA copolymer graftings: generation, protein resistance, and a hydrophobic domain. Langmuir 2008;24:8151–7.

[31] Yoshikawa C, Goto A, Tsujii Y, Fukuda T, Kimura T, Yamamoto K, et al. Protein repellency of well-defined, concentrated poly(2-hydroxyethyl methacrylate) brushes by the size-exclusion effect. Macromolecules 2006;39:2284–90.

[32] Fan XW, Lin LJ, Messersmith PB. Cell fouling resistance of polymer brushes grafted from Ti substrates by surface-initiated polymerization: effect of ethylene glycol side chain length. Biomacromolecules 2006;7:2443–8.

[33] Lee SB, Koepsel RR, Morley SW, Matyjaszewski K, Sun YJ, Russell AJ. Permanent, nonleaching antibacterial surfaces: 1. Synthesis by atom transfer radical polymerization. Biomacromolecules 2004;5:877–82.

[34] Janzen J, Le Y, Kizhakkedathu JN, Brooks DE. Plasma protein adsorption to surfaces grafted with dense homopolymer and copolymer brushes containing poly(N-isopropylacrylamide). J Biomater Sci Polym Ed 2004;15:1121–35.

[35] Kizhakkedathu JN, Janzen J, Le Y, Kainthan RK, Brooks DE. Poly(oligo(ethylene glycol)acrylamide) brushes by surface initiated polymerization: effect of macromonomer chain length on brush growth and protein adsorption from blood plasma. Langmuir 2009;25:3794–801.

[36] Lai BFL, Creagh AL, Janzen J, Haynes CA, Brooks DE, Kizhakkedathu JN. The induction of thrombus generation on nanostructured neutral polymer brush surfaces. Biomaterials 2010;31:6710–8.

[37] Yameen B, Alvarez M, Azzaroni O, Jonas U, Knoll W. Tailoring of poly(ether ether ketone) surface properties via surface-initiated atom transfer radical polymerization. Langmuir 2009;25:6214–20.

[38] Savina IN, Cnudde V, D'Hollander S, Van Hoorebeke L, Mattiasson B, Galaev IY, et al. Cryogels from poly(2-hydroxyethyl methacrylate): macroporous, interconnected materials with potential as cell scaffolds. Soft Matter 2007;3:1176–84.

[39] Lokuge I, Wang X, Bohn PW. Temperature-controlled flow switching in nanocapillary array membranes mediated by poly(N-isopropylacrylamide) polymer brushes grafted by atom transfer radical polymerization. Langmuir 2007;23:305–11.

[40] Xu FJ, Zhao JP, Kang ET, Neoh KG, Li J. Functionalization of nylon membranes via surface-initiated atom-transfer radical polymerization. Langmuir 2007;23:8585–92.

[41] Bruening ML, Dotzauer DM, Jain P, Ouyang L, Baker GL. Creation of functional membranes using polyelectrolyte multilayers and polymer brushes. Langmuir 2008;24:7663–73.

[42] Kaur S, Ma Z, Gopal R, Singh G, Ramakrishna S, Matsuura T. Plasma-induced graft copolymerization of poly(methacrylic acid) on electrospun poly(vinylidene fluoride) nanofiber membrane. Langmuir 2007;23:13085–92.

[43] Schepelina O, Zharov I. Poly(2-(dimethylamino)ethyl methacrylate)-modified nanoporous colloidal films with pH and ion response. Langmuir 2008;24:14188–14194.

[44] Nagase K, Kobayashi J, Kikuchi A, Akiyama Y, Annaka M, Kanazawa H, et al. Influence of graft interface polarity on hydration/dehydration of grafted thermoresponsive polymer brushes and steroid separation using all-aqueous chromatography. Langmuir 2008;24:10981–7.

[45] Nagase K, Kobayashi J, Kikuchi AI, Akiyama Y, Kanazawa H, Okano T. Effects of graft densities and chain lengths on separation of bioactive compounds by nanolayered thermoresponsive polymer brush surfaces. Langmuir 2008;24:511–7.

[46] Leinweber FC, Stein J, Otto M. Capillary zone electrophoresis of proteins with poly(2-hydroxyethyl methacrylate)-coated capillaries: fundamentals and applications. Fresenius J Anal Chem 2001;370:781–8.

[47] Miller MD, Baker GL, Bruening ML. Polymer-brush stationary phases for open-tubular capillary electrochromatography. J Chromatogr A 2004;1044:323–30.

[48] Unsal E, Elmas B, Caglayan B, Tuncel M, Patir S, Tuncel A. Preparation of an ion-exchange chromatographic support by a "grafting from" strategy based on atom transfer radical polymerization. Anal Chem 2006;78:5868–75.

[49] Coad BR, Steels BM, Kizhakkedathu JN, Brooks DE, Haynes CA. The influence of grafted polymer architecture and fluid hydrodynamics on protein separation by entropic interaction chromatography. Biotechnol Bioeng 2006;97:574–87.

[50] Coad BR, Kizhakkedathu JN, Haynes CA, Brooks DE. Synthesis of novel size exclusion chromatography support by surface initiated aqueous atom transfer radical polymerization. Langmuir 2007;23:11791–803.

[51] Hucknall A, Rangarajan S, Chilkoti A. In pursuit of zero: polymer brushes that resist the adsorption of proteins. Adv Mater 2009;21:2441–6.

[52] Jiang XW, Chen HY, Galvan G, Yoshida M, Lahann J. Vapor-based initiator coatings for atom transfer radical polymerization. Adv Funct Mater 2008;18:27–35.

[53] Teare DOH, Schofield WCE, Garrod RP, Badyal JPS. Poly(N-acryloylsarcosine methyl ester) protein-resistant surfaces. J Phys Chem B 2005;109:20923–8.
[54] Teare DOH, Barwick DC, Schofield WCE, Garrod RP, Beeby A, Badyal JPS. Functionalization of solid surfaces with thermoresponsive protein-resistant films. J Phys Chem B 2005;109:22407–12.
[55] Teare DOH, Schofield WCE, Garrod RP, Badyal JPS. Rapid polymer brush growth by TEMPO-mediated controlled free-radical polymerization from swollen plasma deposited poly(maleic anhydride) initiator surfaces. Langmuir 2005;21:10818–24.
[56] Teare DOH, Barwick DC, Schofield WCE, Garrod RP, Ward LJ, Badyal JPS. Substrate-independent approach for polymer brush growth by surface atom transfer radical polymerization. Langmuir 2005;21:11425–30.
[57] Edmondson S, Armes SP. Synthesis of surface-initiated polymer brushes using macro-initiators. Polym Int 2009;58:307–16.
[58] Edmondson S, Vo C-D, Armes SP, Unali G-F. Surface polymerization from planar surfaces by atom transfer radical polymerization using polyelectrolytic macroinitiators. Macromolecules 2007;40:5271–8.
[59] Chen XY, Armes SP, Greaves SJ, Watts JF. Synthesis of hydrophilic polymer-grafted ultrafine inorganic oxide particles in protic media at ambient temperature via atom transfer radical polymerization: use of an electrostatically adsorbed polyelectrolytic macroinitiator. Langmuir 2004;20:587–95.
[60] Meagher L, Thissen H, Pasic P, Evans RA, Johnson G. Method for controllably locating polymerization initiators on substrate surface for forming biological coating involves covalently binding macromolecule to surface having several polymerization initiators and several surface binding groups. Commonwealth Sci Ind Res Org (Csir); 2008. p. 2052045-A1.
[61] Griesser HJ. Small scale reactor for plasma processing of moving substrate web. Vacuum 1989;39:485–8.
[62] Tanuma S, Powell CJ, Penn DR. Calculations of electron inelastic mean free paths (IMFPS): 4. Evaluation of calculated IMFPS and of the predictive IMFP formula TPP-2 for electron energies between 50 and 2000 eV. Surf Interface Anal 1993;20:77–89.
[63] Vermette P, Meagher L. Immobilization and characterization of poly(acrylic acid) graft layers. Langmuir 2002;18:10137–45.
[64] Short RD, Goruppa A. Plasma polymerisation: improved mechanistic understanding of deposition, new materials and applications. In: Ryan AJ, editor. Emerging themes in polymer science. London: The Royal Society of Chemistry; 2001. p. 119–33.
[65] Vasilev K, Michelmore A, Griesser HJ, Short RD. Substrate influence on the initial growth phase of plasma-deposited polymer films. Chem Commun 2009:3600–2.
[66] Siow KS, Britcher L, Kumar S, Griesser HJ. Plasma methods for the generation of chemically reactive surfaces for biomolecule immobilization and cell colonization – a review. Plasma Processes Polym 2006;3:392–418.
[67] Ratner BD, Bryant SJ. Biomaterials: where we have been and where we are going. Annu Rev Biomed Eng 2004;6:41–75.
[68] de Gennes PG. Conformations of polymers attached to an interface. Macromolecules 1980;13:1069–75.
[69] Norde W, Lyklema J. The adsorption of human-plasma albumin and bovine pancreas ribonuclease at negatively charged polystyrene surfaces: 1. Adsorption isotherms. Effects of charge, ionic-strength, and temperature. J Colloid Interface Sci 1978;66:257–65.
[70] Pasche S, Textor M, Meagher L, Spencer ND, Griesser HJ. Relationship between interfacial forces measured by colloid-probe atomic force microscopy and protein resistance of poly(ethylene glycol)-grafted poly(L-lysine) adlayers on niobia surfaces. Langmuir 2005;21:6508–20.
[71] Zhao C, Li L, Wang Q, Yu Q, Zheng J. Effect of film thickness on the antifouling performance of poly(hydroxy-functional methacrylates) grafted surfaces. Langmuir 2011;27:4906–13.
[72] Halperin A. Polymer brushes that resist adsorption of model proteins: design parameters. Langmuir 1999;15:2525–33.
[73] Unsworth LD, Sheardown H, Brash JL. Protein-resistant poly(ethylene oxide)-grafted surfaces: chain density-dependent multiple mechanisms of action. Langmuir 2008;24:1924–9.